Applied Thermal Engineering 53 (2013) 147–156

Contents lists available at SciVerse ScienceDirect

Applied Thermal Engineering

journal homepage: www.elsevier.com/locate/apthermeng

Internal and external fin heat transfer enhancement technique for latent heat thermal energy storage in triplex tube heat exchangers

Abduljalil A. Al-Abidi [a,b,*], Sohif Mat [a], K. Sopian [a], M.Y. Sulaiman [a], Abdulrahman Th. Mohammad [a]

[a] Solar Energy Research Institute, University Kebangsaan Malaysia, Bangi, Selangor, Malaysia
[b] Department of HVAC Engineering, Sana'a Community College, P.O. Box 5695, Sana'a, Yemen

HIGHLIGHTS

► The melting time of the PCM minimized by using TTHX with internal and external fins.
► The temperature difference between the HTF and the PCM was around (3–8 °C) only.
► Different design configurations of the TTHX to melt the PCM were used.
► The melting time for Case G (8-cells unit geometry) is reduced to about 34.7%.

ARTICLE INFO

Article history:
Received 29 May 2012
Received in revised form
9 January 2013
Accepted 10 January 2013
Available online 28 January 2013

Keywords:
Melting
Phase change material
Triplex tube heat exchanger
Heat transfer enhancement

ABSTRACT

The importance of latent heat thermal energy storage is significant in contrast to sensible energy storage because of the large storage energy densities per unit mass/volume at nearly constant thermal energy. In this paper, heat transfer enhancement technique by using internal and external fins for PCM melting in a triplex tube heat exchanger (TTHX) was investigated numerically. A two-dimensional numerical model is developed using the Fluent 6.3.26 software program, and pure conduction and natural convection are considered in the simulation. The number of fins, fin length, fin thickness, Stefan number, TTHX material, and the phase change material (PCM) unit geometry in the TTHX are found to influence the time for complete melting of the PCM. Experiments were conducted to validate the proposed model. Simulated results agree with the experimental results. The computational results show that case G (8-cell PCM unit geometry) achieved a shorter time in completing the melting of the PCM, the total melting time is decreased to 34.7%.

1. Introduction

It is becoming increasingly difficult to ignore the mismatch between the energy supply and energy demand for solar thermal energy applications, since solar energy is considered as a periodic energy source, which leads to low efficiency of those applications. Latent heat thermal energy storage is an important component and plays a key role in the energy efficiency improvement of the solar-energy applications. Recently, thermal energy storage systems, especially latent heat thermal energy storage, have gained a greater attention from the viewpoint of global environmental problems and the energy-efficiency improvement. It promises an elevated performance and reliability with the advantages of high storage density and nearly constant thermal energy [1]; the using of phase change materials (PCM) can be found in different engineering fields, such as thermal storage of a building structure [2–5], building equipment such as domestic hot water, heating and cooling systems [6,7], electronic products [8,9], drying technology [10], waste heat recovery [11], refrigeration and cold storage [12,13], solar air collector [14], and solar cookers [15].

The main disadvantages of PCMs that limit the using of these materials as thermal energy storage is the low thermal conductivity, which causes a long time for the melting and solidification process. Several researchers have studied the heat transfer enhancement in PCMs, including finned tubes [16,17], insertion of a metal matrix to the PCM [18,19], using multitubes [20], using bubble agitation in PCMs [21], using a PCM dispersed with high conductivity particles, and employing multiple families of PCMs [22,23].

Most researchers reported that the increase of the heat transfer area will lead to improve the heat transfer between the heat

* Corresponding author. Department of HVAC Engineering, Sana'a Community College, P.O. Box 5695, Sana'a, Yemen. Tel.: +60 147169139; fax: +60 389214593.
E-mail addresses: abo_anas4@yahoo.com, duljalil17@gmail.com (A.A. Al-Abidi).

1359-4311/$ – see front matter © 2013 Elsevier Ltd. All rights reserved.
http://dx.doi.org/10.1016/j.applthermaleng.2013.01.011

transfer fluid (HTF) and the PCM. The majority of the heat enhancement techniques have been based on the application of fins embedded in the PCM; this is probably due to their simplicity, ease in fabrication, and low cost of construction [24]. There are different fin configurations applied to the PCMs, including external fins, and internal fins (circular, longitudinal, rectangular).

Ismail et al. [25] investigated numerically and experimentally the effect of fin design parameters such as the fin length, fin thickness, number of fins, and the aspect ratio of the annular space on the complete solidification, solidified mass fraction, and the total stored energy of the PCM. Agyenim et al. [26] studied the heat transfer enhancement by using different fin configurations (control PCM system, circular fin PCM system, and longitudinal fin PCM system) to improve the heat transfer of the PCM. They recommended that the longitudinal fins are better than the circular fins. Shatikian et al. [27] presented a numerical study of the melting process of the PCM with internal fins opened to air from the top for electronic cooling purposes; they investigated different fin dimensions with a constant ratio between the fin size and the PCM thickness. Wang and Yang [9] studied numerically the cooling technology of portable hand-held electronic devices by using PCM; they developed a 3D simulation model to investigate the effect of a different amount of fins and various heating levels.

Rectangular, uniformly-spaced axial fins have been attached to the inner tube by Padmanabhan and Murthy [28], where the outer tube is considered insulated; they studied theoretically the solidification process in a cylindrical annulus and the influence of different design and operation parameter effects. Stritih [29] used a rectangular external fin to enhance the heat transfer during melting and solidification of a latent heat storage system for thermal application in building purposes; they concluded that heat storage (melting) was not a problem during thermal storage applications, and that the extraction of heat (solidification) can be effectively enhanced with fins.

Velraj et al. [30] investigated numerically and experimentally the effect of internal longitudinal fins on the solidification process of paraffin (RT60) inside a vertical cylinder. They considered the heat transfer through the fin tip and the circumferential wall of the cylinder. The effects of different tube radii and different numbers of fins have been studied theoretically with respect to the surface heat flux on the solidification process of the paraffin. Erek et al. [17] have investigated the behaviour of thermal energy storage (shell and tube type) with circular-finned tube and PCM in the annular space. They developed a 2D numerical model to predict the effect of the fin dimensions and the operation parameters (fin space, fin diameter, Re number, heat transfer fluid inlet temperature) to the solidification and melting process of the PCM, and an experimental unit was designed to compare the numerical and the experimental results. Medrano et al. [31] experimentally investigated the heat-transfer properties, melting (charge), and solidification (discharge) process of paraffin RT35 PCM in a small double-pipe heat exchanger with 13 circular fins and PCM in the annular space.

Balikowski and Mollendorf [32] used a spined pipe tube heat exchanger with two types of PCMs and studied the charging/discharging of a vertical double-pipe heat exchanger with different PCM in the annular gap. As most studies had embedded the fins into the PCM as a result of the PCM's low thermal conductivity, Zhang and Faghri [33] used an internally-finned tube for the HTF, whereas the PCM filled in the annular shell space; the results showed that adding internal fins is an efficient way to enhance the heat transfer in thermal energy storage systems, especially when using a low thermal conductivity like air as an HTF. Velraj et al. [21] examined experimentally three heat transfer enhancement methods in PCMs, which were internal longitudinal fins inside a cylindrical vertical tube containing paraffin, filled tube with lessing steel rings (1 cm) diameter, and creating bubble agitation inside the PCM. They recommended that the heat transfer enhancement by using fins is appreciable and highly suitable for solidification enhancement.

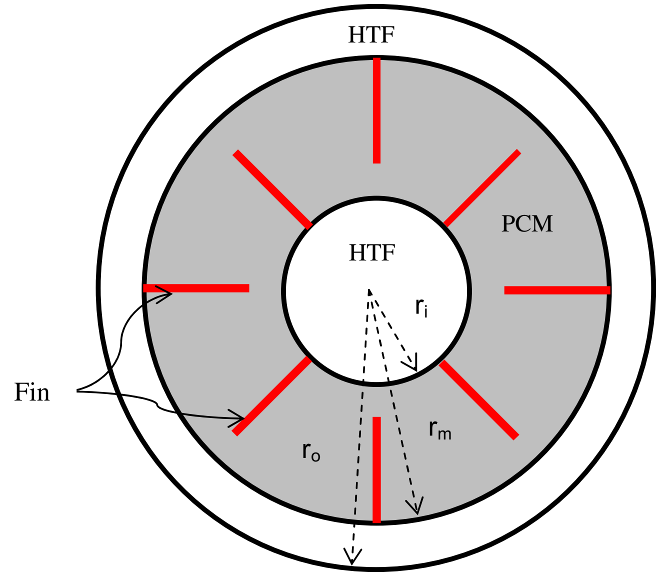

Fig. 1. The physical configuration of the TTHX.

Triplex tube heat exchanger (TTHX) is used in various products and are found in the dairy, food, beverage, and pharmaceutical industries [34]. TTHX with PCM in the middle tubes increases the heat-transfer area, consequently improving the heat transfer relative to that of the double pipe heat exchanger. In addition, the time required for total melting and the inlet temperature for the HTF are reduced. In the present work, the effect of longitudinal external and internal fins in the TTHX is investigated numerically; the number of fins, fin length, fin thickness, TTHX materials were investigated, the PCM unit geometries in the TTHX were developed and their effect on the melting process was studied. Finally, Stefan number was studied to improve the performance of the PCM thermal energy storage.

2. Numerical approach

2.1. Physical model

The physical configuration of the TTHX is shown in Fig. 1, the inner tube radius (r_i) is 25.4 mm with 1.2 mm thickness, the middle tube radius (r_m) is 75 mm and the outer tube radius (r_o) is 100 mm; with 2 mm thickness, all pipes are made from copper to ensure high thermal conductivity and to enhance heat transfer between the PCM and the HTF. Different numbers of fins were incorporated to the TTHX for cases A, B, C, and D are listed in Table 1. Fin's length was extended to fill the gap between the inner and the middle tubes. The fin was welded to the tubes to create a separate PCM unit geometry to fill with PCM. Table 2 lists the different number of PCM unit geometries cases E, F, and G as shown in Fig. 2. The fin length and fin thickness parameters of case D were investigated in detail. All cases are summarized in Tables 1–3. The outer and inner tubes were used for the HTF, whereas the middle tube was used for the PCM. The PCM

Table 1
Number of fins for TTHX.

Cases	No. of fins	Fin length (mm)	Fin thickness (mm)
Case A	–	–	–
Case B	4	42	1
Case C	6	42	1
Case D	8	42	1

Table 2
Cell geometry variation for the TTHX.

Case	No. of cell (PCM unit geometry)	Fin length (mm)	Fin thickness (mm)
Case E	4	47.6	1
Case F	6	47.6	1
Case G	8	47.6	1

was based on a commercially available material, RT82 (Rubitherm GmbH-Germany). The thermo-physical properties of RT82 are listed in Table 4. This thermal energy storage delivered the thermal energy required by a liquid desiccant air-conditioning system. Water was used as HTF. The minimum temperature required to operate the liquid desiccant air conditioning was approximately 65 °C. Water was used as HTF because of its high heat capacity and low cost, so the maximum charging temperature was 95 °C which equivalent to 13 °C temperature difference between the PCM and the HTF.

2.2. Governing equation

For the mathematical equation of the melting process of the PCM inside the middle tube of the TTHX, the following assumptions are made:

Table 3
Fin length and fin thickness variations for TTHX.

Case	No. of fins	Fin length (mm)	Fin thickness (mm)
Case D	8	10	1
	8	20	1
	8	30	1
	8	42	1
	8	42	2
	8	42	3
	8	42	4

- The flow is laminar, unsteady, and incompressible.
- The viscous dissipation is considered negligible.
- The effect of natural convection during melting is considered by invoked the Boussinesq approximation which is valid for the density variations buoyancy force, otherwise they are neglected.
- The thermo-physical properties of the HTF and PCMs are independent of the temperature;

The continuity, momentum, and thermal energy equations can be written as [35]:

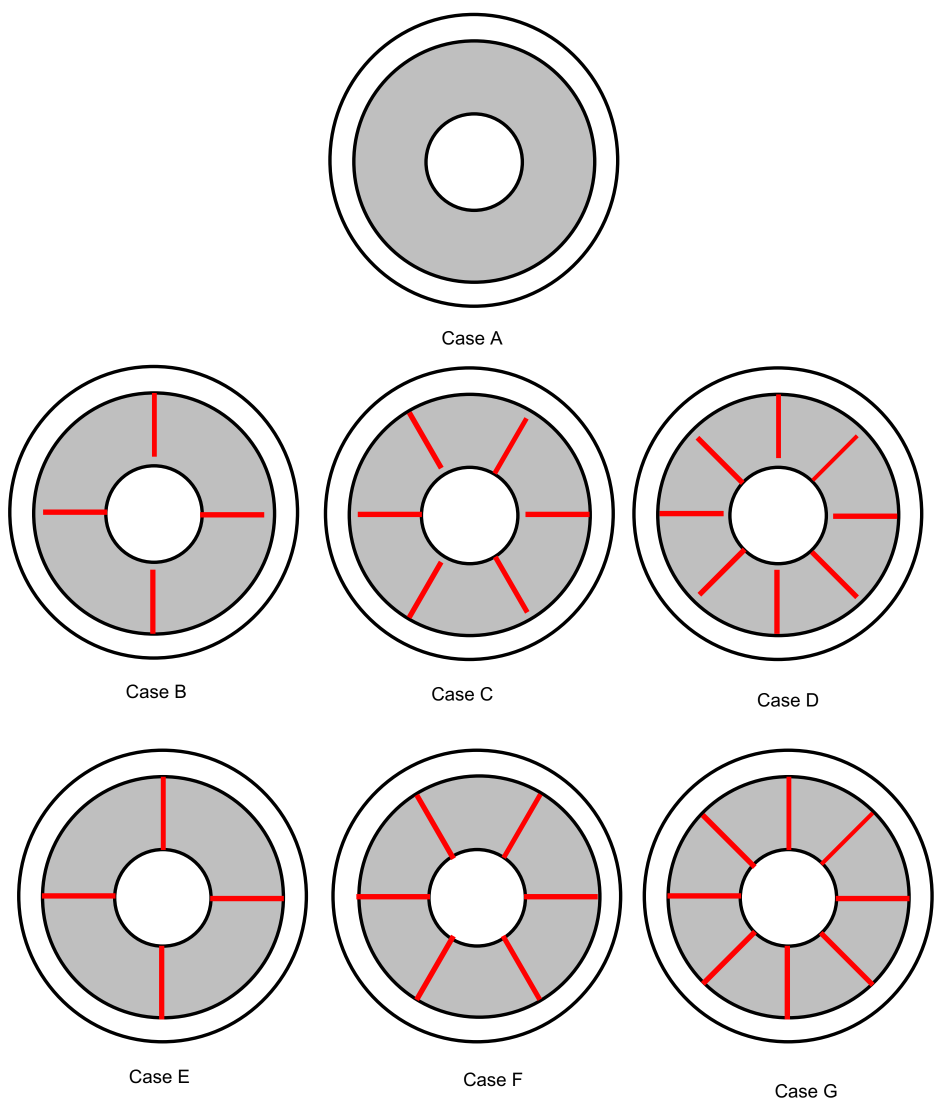

Fig. 2. Physical configurations of all cases.

Table 4
Thermo-physical properties of the PCM.

Property	RT82
Density of PCM, solid, ρ_s (kg/m^3)	950
Density of PCM, liquid, ρ_l (kg/m^3)	770
Specific heat of PCM, liquid, Cp_l, Cp_s (J/kg K)	2000
Latent heat of fusion, L (J/kg)	176000
Melting temperature, T_m (K)	350.15–358.15
Thermal conductivity, k (W/m K)	0.2
Thermal expansion coefficient (1/K)	0.001
Dynamic Viscosity, μ (kg/m s)	0.03499

Continuity:

$$\partial_t(\rho) + \partial_i(\rho u_i) = 0 \tag{1}$$

Momentum:

$$\partial_t(\rho u_i) + \partial_i(\rho u_i u_j) = \mu\partial_{jj}u_i - \partial_i p + \rho g_i + S_i \tag{2}$$

The energy equation:

$$\partial_t(\rho h) + \partial_t(\rho\Delta H) + \partial_i(\rho u_i h) = \partial_i(k\partial_i T) \tag{3}$$

Where ρ is the density of PCM (RT82),u_i is the fluid velocity, μ is the dynamic viscosity, p is the pressure, g is the gravity acceleration, k is the thermal conductivity, and h is the sensible enthalpy.

The sensible enthalpy can be expressed as:

$$h = h_{ref} + \int_{T_{ref}}^{T} cp\, dT \tag{4}$$

The enthalpy, H, can be defined as:

$$H = h + \Delta H \tag{5}$$

Where h_{ref} is the reference enthalpy at the reference temperature T_{ref}, cp is the specific heat, ΔH is the latent heat content that may change between zero (solid) and L (liquid), the latent heat of the PCM, and β is the liquid fraction that happens during the phase change between the solid and liquid state when the temperature is $T_l > T > T_s$, and can be written as:

$$\beta = \Delta H/L \tag{6}$$

$$\beta = \begin{cases} 0 & \text{if} \quad T < T_s \\ 1 & \text{if} \quad T > T_l \\ (T - T_s)/(T_l - T_s) & \text{if} \quad T_l > T > T_s \end{cases} \tag{7}$$

The sources term S_i in the momentum equation, Eq. (2), is defined as:

$$S_i = C(1-\beta)^2 \frac{u_i}{\beta^3 + \varepsilon} \tag{8}$$

Where $C\,(1-\beta)^2/\beta^3 + \varepsilon$ is the "porosity function" defined by Brent et al. [36] to make the momentum equations "mimic" Carmane Kozeny equations for flow in porous media. C is a constant reflect of the mushy zone morphology. It describes how steeply the velocity is reduced to zero when the material solidifies, this constant is varied between 10^4–10^7, so 10^5 is considered for this work [37]. ε is a small number (0.001) to prevent division by zero.

2.3. Initial and boundary condition

At the initial time, the PCM was considered as solid state, and the temperature was 300.15 K, whereas the constant temperature of the tube wall represented the HTF temperature, which were

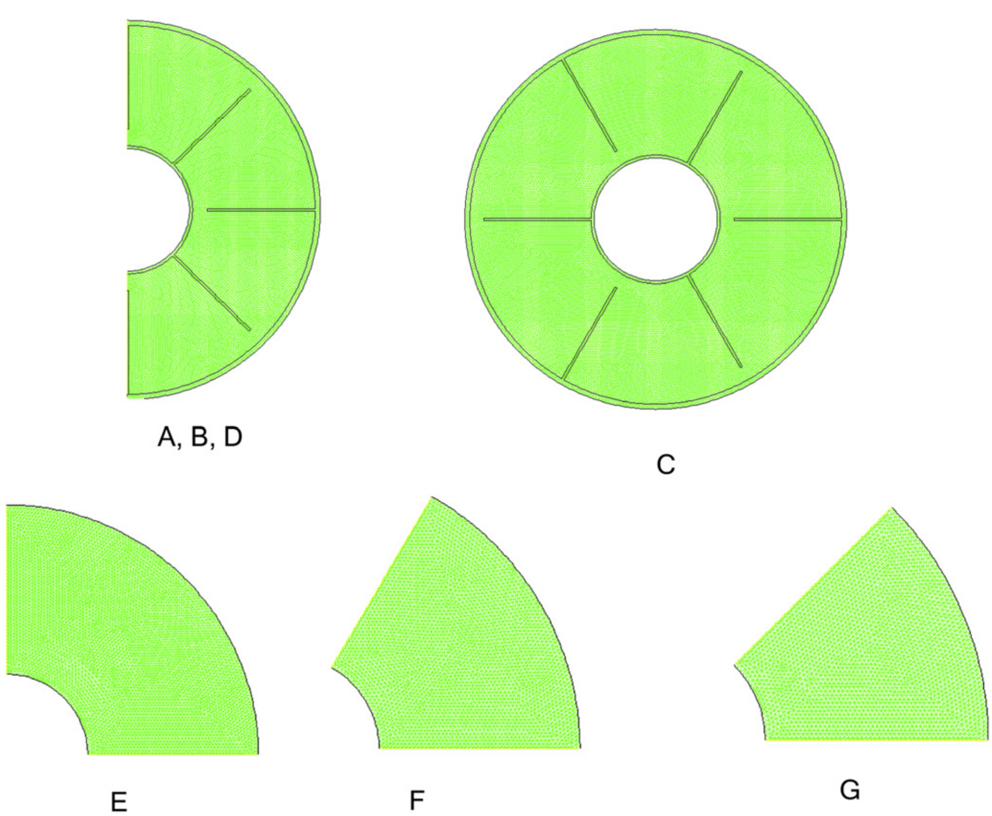

Fig. 3. Computational grids for all cases in TTHX.

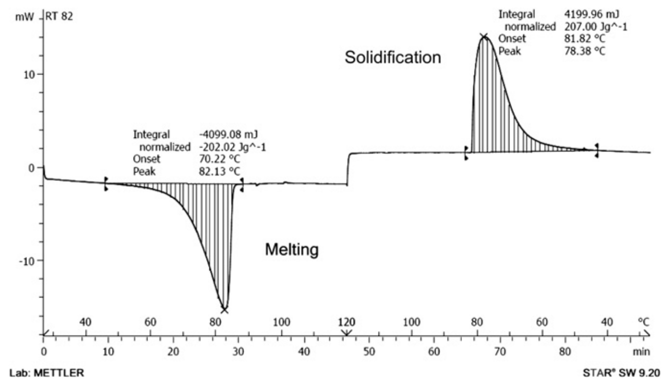

Fig. 4. DSC curves RT 82 PCM cooling and heating rate: 2 °C/min.

358.15 K, 360.15 K, and 363.15 K, respectively.The boundary conditions of the TTHX can be written as below;

$$\text{at } r = r_i \rightarrow T = T_{HTF} \tag{9}$$

$$\text{at } r = r_m \rightarrow T = T_{HTF} \tag{10}$$

The initial temperature for the three models will be

$$\text{at } t = 0 \rightarrow T = T_{ini} \tag{11}$$

2.4. Numerical modelling

The modelling has been conducted by using FLUENT software which depends on the enthalpy-porosity technique and on the finite volume methods as the described by Patankar [38]. In the former, the melt interface is not tracked explicitly. A quantity called liquid fraction, which indicates the fraction of the cell volume in liquid form, is associated with each cell in the domain. The liquid fraction is computed at each iteration based on enthalpy balance. The mushy zone is a region wherein the liquid fraction lies between 0 and 1. The mushy zone is modeled as a "pseudo" porous medium in which the porosity decreases from 1 to 0 as the material solidifies. When the material has fully solidified in a cell, the porosity becomes zero, resulting in the drop of velocities to zero. For details on the CFD application in the latent heat thermal energy storage, refer to [39].

A commercial computational program (FLUENT 6.3.26), solidification and melting models, were used to simulate the melting process of the PCM. Two TTHX dimensions (r, θ) were drawn and meshed in a geometric model. The mesh generation software Gambit, combined with the FLUENT software, helped define the boundary layers and zone types. The mesh was then exported to FLUENT. Different computational grids were adopted for the different cases to reduce simulation time. Half-sections were used for cases A, B, and D, whereas a full section was used for case C. Cross-sections were adopted for cases E, F, and G, as shown in Fig. 3.

The PRESTO scheme is used for the pressure correction equation and a well-known Semi-Implicit Pressure-Linked Equation (SIMPLE) algorithm is used for the pressure–velocity coupling; the under relaxation value factors for pressure, velocity, energy, and liquid fraction are 0.3, 0.2, 1, and 0.9, respectively. The independency of the time steps from the melt fraction was examined for the simulations at 1 s, 0.5 s(chosen), and 0.2 s. In addition, three grid sizes of 17956 (chosen), 22004, and 27854 cells were investigated to validate the independency of the grid size from the numerical solution. Using 17956 cells with a 0.5 s time step was considered for our calculation, which were used to achieve the predetermined convergence of energy equation (10^{-5}) and 10^{-3} for the velocities.

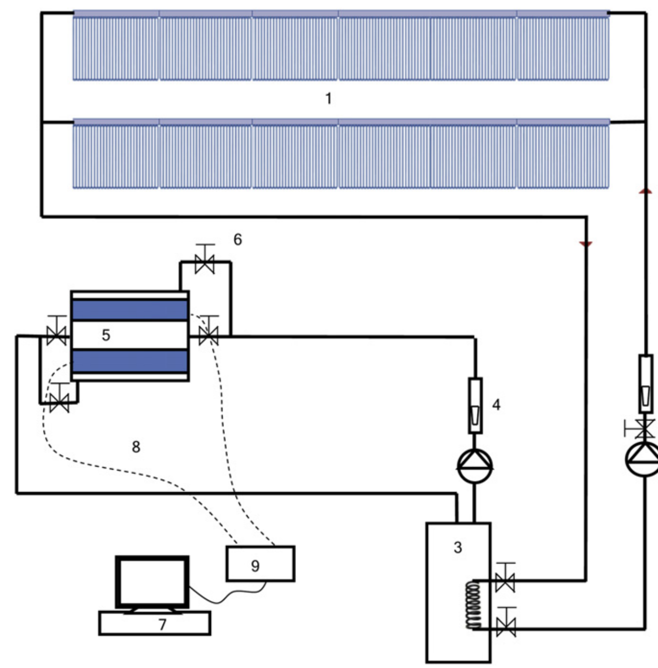

Fig. 5. Schematic diagram of the experimental apparatus which includes an evacuated tube solar collector (1), hot-water circulation pumps (2), charging storage tank with electric heater (3), rotameter to measure the flow rate (4), a triplex concentric tube's heat exchanger (5), manual shit off valve (6), personal computer (7), thermocouples (8), and data logger (9).

3. Validation of the model

3.1. Phase change materials

RT 82 (RUBITHERM GmbH-Germany) with 82 °C melting temperature has been chosen for our application, which satisfies the minimum temperature required for liquid desiccant cooling system, which is in the range of 65 °C–70 °C. Table 4 presents the thermophysical properties of the PCM (data provided by the manufacturer). Approximately 20.29 mg of RT 82 was used for testing the thermal properties of RT 82 (heat of fusion, melting temperature, and solidification temperature). A total of 10 tests for thermal cycling were performed for the same sample. The material was heated from an ambient temperature of 27 °C to a maximum temperature of 120 °C at 2 °C/min. PCM cooling occurred from 120 °C or lower, at the same rate to the ambient temperature. The latent heat of fusion and the melting temperature were measured by differential scanning calorimetry (METTLER TOLEDO-Model

Table 5
Reported of mean and standard uncertainty of the PCM thermal properties.

Melting process			Solidification process		
Onset point (°C)	Peak point (°C)	Heat of fusion (KJ/kg)	Onset point (°C)	Peak point (°C)	Heat of fusion (KJ/kg)
70.1275 ± 0.148172	82.17625 ± 0.047953	201.64375 ± 1.386656	81.86 ± 0.02828	78.158 ± 0.090358	207.807 ± 1.359165

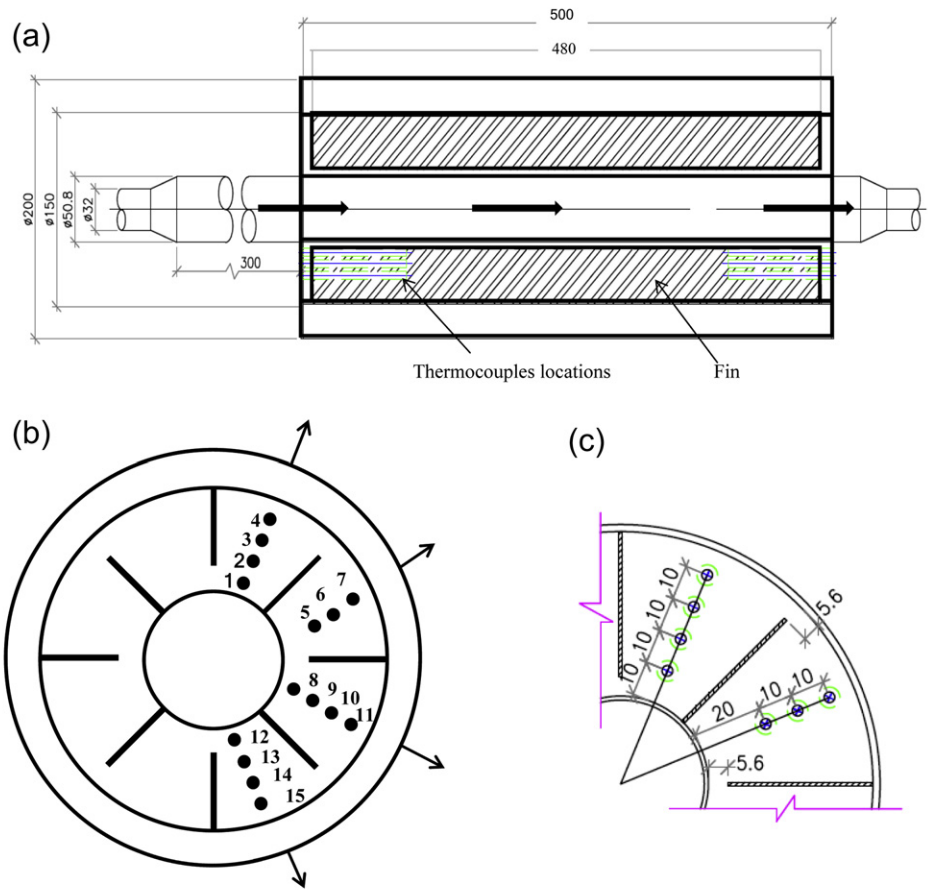

Fig. 6. Schematic diagram of the TTHX; (a) Cross section of TTHX, (b) Thermocouples distributions in TTHX, (c) Radial interval in the radial direction.

DSC1). Fig. 4 shows the relationship between temperature and heat flux in the sample for PCM melting and solidification. Table 5 shows the average results and the standard uncertainty of the melting and freezing temperatures of the material as well as the latent heat of fusion during the melting and freezing process.

3.2. Experimental apparatus and procedure

A triplex concentric tube latent heat thermal storage was fabricated to validate the numerical model of the PCM melting process. Fig. 5 shows a schematic diagram of the experimental apparatus, which includes TTHX, hot-water circulation pumps, evacuated tube solar collector, charging storage tank with electric heater, rotameter for measuring the flow rate, and manual shit off valves. Fig. 6 shows the TTHX section consisting of three horizontally mounted concentric tubes with lengths of 500 mm and four longitudinal fins (fin pitch of 42 mm, length of 480 mm, and thickness of 1 mm) welded to each of the inner and middle tubes. The physical geometrical parameters of the TTHX are mentioned in the physical model section. The inner tube was extended to approximately 300 mm from the entrance to ensure that the flow will be fully developed. The data monitoring system comprised K-type thermocouples (measured at

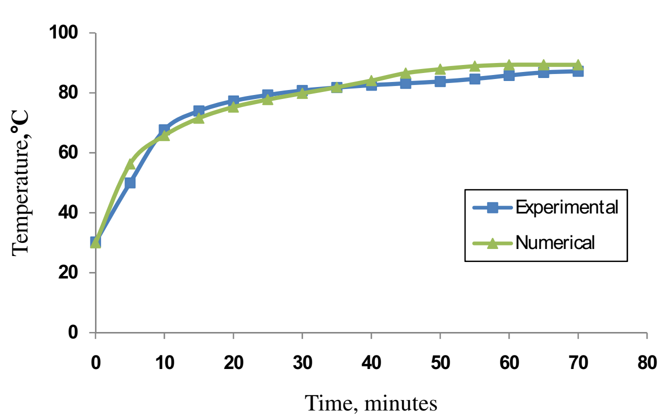

Fig. 7. Comparison of the experimental and numerical average temperature versus time.

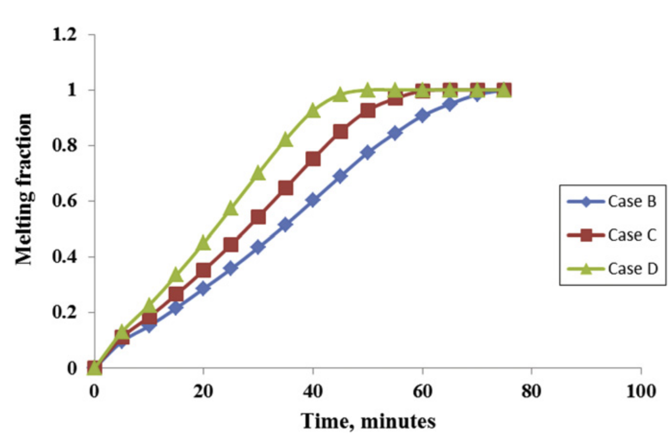

Fig. 8. Number of fin effect to the melting time.

Table 6
The melting time percentage for different cases of TTHX (%).

A	B	C	D	E	F	G
100	69.5	56.5	43.4	52	39	34.7

0.5% accuracy), a data logger, and a personal computer to measure the temperatures in the PCM thermal storage. The HTF flow rate was measured by a rotameter (measured at 5% accuracy).

A total of 15 thermocouples have emerged in the PCM at 10 mm intervals fitted in radial and different angular directions, located 100 mm from the entrance of the HTF in the thermal storage, as shown in Fig. 6. The PCM thermal storage is wrapped with a 70 mm thick glass wool insulation to decrease heat loss and achieve an adiabatic surface.

The hot water used in the charging process was delivered from a central heating station of the Green Technology Park at the Solar Research Energy Institute, National University of Malaysia, as shown in Fig. 5. This heating station was designed to deliver the hot water required by various solar thermal systems. The central heating station consists of 300 evacuated tube solar collectors with three 200 L storage tanks. One storage tank was used for the current application. The TTHX was filled with 5.6 kg liquid PCM; no leakage was observed. Charging started when the storage tank reached a temperature 90 °C.

3.3. Validation of the numerical model

The numerical model of melting created using Fluent 6.3.26 software was compared with an experiment to validate the numerical model. The average temperature of the PCM was 27 °C when the melting process started, whereas the HTF temperature was 90 °C, which was maintained in the storage tank by using an electrical heater and a thermostat controller. The mass flow rate of the HTF was 8.3 l/min. The melting range of the PCM depended on the experimental test, which was between 70 °C and 82 °C. Fig. 7 shows the comparison of the average temperature versus time of PCM, which was collected using the 15 thermocouples inserted in the PCM at the HTF tube entrance, with that of the numerical model. The results of the present model showed an acceptable agreement with the experimental results.

4. Results and discussion

4.1. The effect of number of fins on the melting rate

Fig. 8 shows the effect of the number of fins on the melting fraction of the PCM for cases A, B, C, and D. Different numbers of fins were studied, as summarized in Table 1. It can be seen that the melting time of PCM was decreased with the increasing in the number of fins. The complete melting time for Cases B, C, and D were 69.5%, 56.5%, and 43.4% of that of the TTHX without fin (Case A) respectively as reported in Table 6. There has been a big influence of the number of fins on the melting fraction at any given time, and it can be considered that this effect is greater for a large number of fins, which means this parameter has a significant effect on the PCM melting process; this is because the fins extend the heat transfer area and conduct the heat directly to the PCM surfaces.

Table 7
The melting time percentage for case D in TTHX with respect to Case A (%).

Case A	Case D							
	Fin length (mm)				Fin thickness (mm)			
	10	20	30	42	1	2	3	4
100	73.9	60.8	47.8	43.4	43.4	39	39	35

4.2. The effect of fin length and fin thickness on the melting fraction

Fig. 9 presents the effect of the fin length on the melting time for case D. One can observe that the melting time decreased when the fin length increased. Table 7 compares the results obtained from the numerical model of melting time percentage of the fins length with respect to case A. It is apparent from this table that the fin length has a significant effect on the melting time. The time

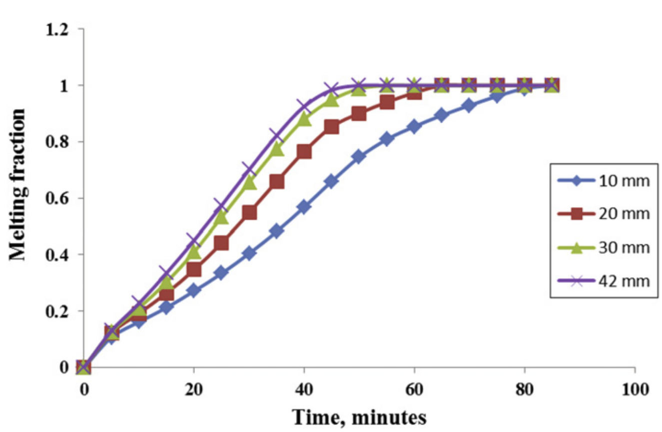

Fig. 9. Fin length effect to the melting time.

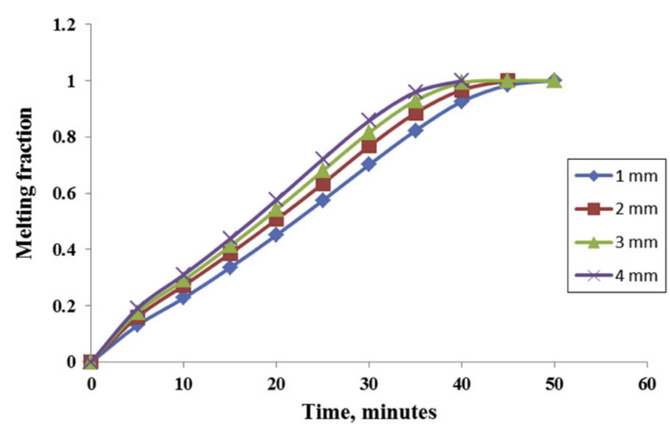

Fig. 10. Fin thickness effect to the melting time.

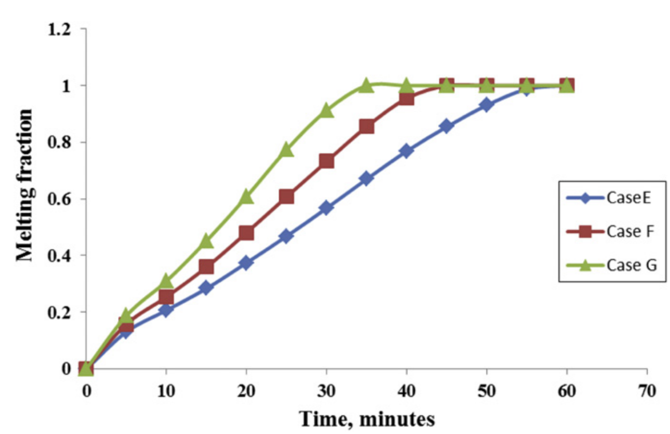

Fig. 11. PCM unit geometry effect to the melting time.

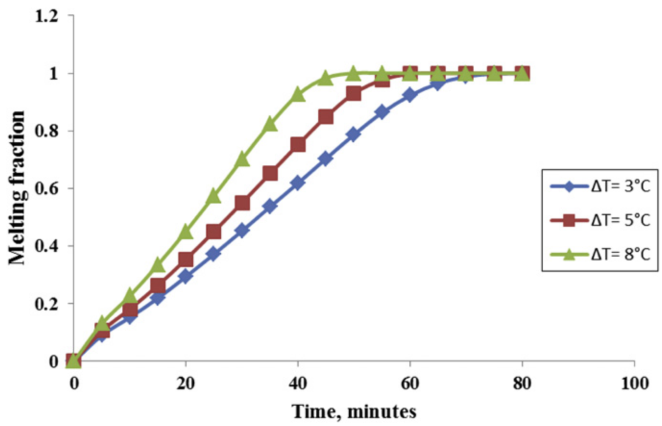

Fig. 12. Stefan number effect to the melting time.

required to complete melting for fin length of 10 mm, 20 mm, 30 mm, 42 mm were 73.9%, 60.8%,47.8%, and 43.4% respectively of the case A.

Fig. 10 shows the influence of the fin thickness on the melting time for case D. As shown in Fig. 10, the increase in fin thickness leaded to the decrease of the melting time. One can also observe that the effect of the fin thickness is small. Table 7 shows that there was no a significant difference on the melting time when the fin thickness changed from 1 mm to 4 mm. The time required to complete melting for fin thickness of 1 mm, 2 mm, 3 mm, 4 mm were 43.4%, 39%, 39%, and 35% respectively of the case A. It can be concluded that there is little effect of the fin thickness on the melting process; their effect was totally close together when the thickness increased. It is desirable to have thin fins for better performance in latent heat thermal energy storage as reported by Padmanabhan and Murthy [28].

4.3. Influence of the PCM unit geometric in the TTHX

In order to show the differences in the melting process for different PCM unit geometries are shown in detail for case E, F, G in Fig. 11. It is illustrated how the melting rate and heat transfer are affected by the geometry of the PCM units in the TTHX. The time required for melting decreased with increasing number of PCM unit geometries as indicated in Table 6. Case G completed the melting process of the PCM in 34.7% of case A, which is considered the shortest time for all cases. It can be concluded that the PCM unit geometry has significant influence on the melting rate; this is because the fins extend the heat transfer area and conduct heat directly to the PCM surfaces and the natural convection remains inside the unit, which accelerates the melting process in each cell.

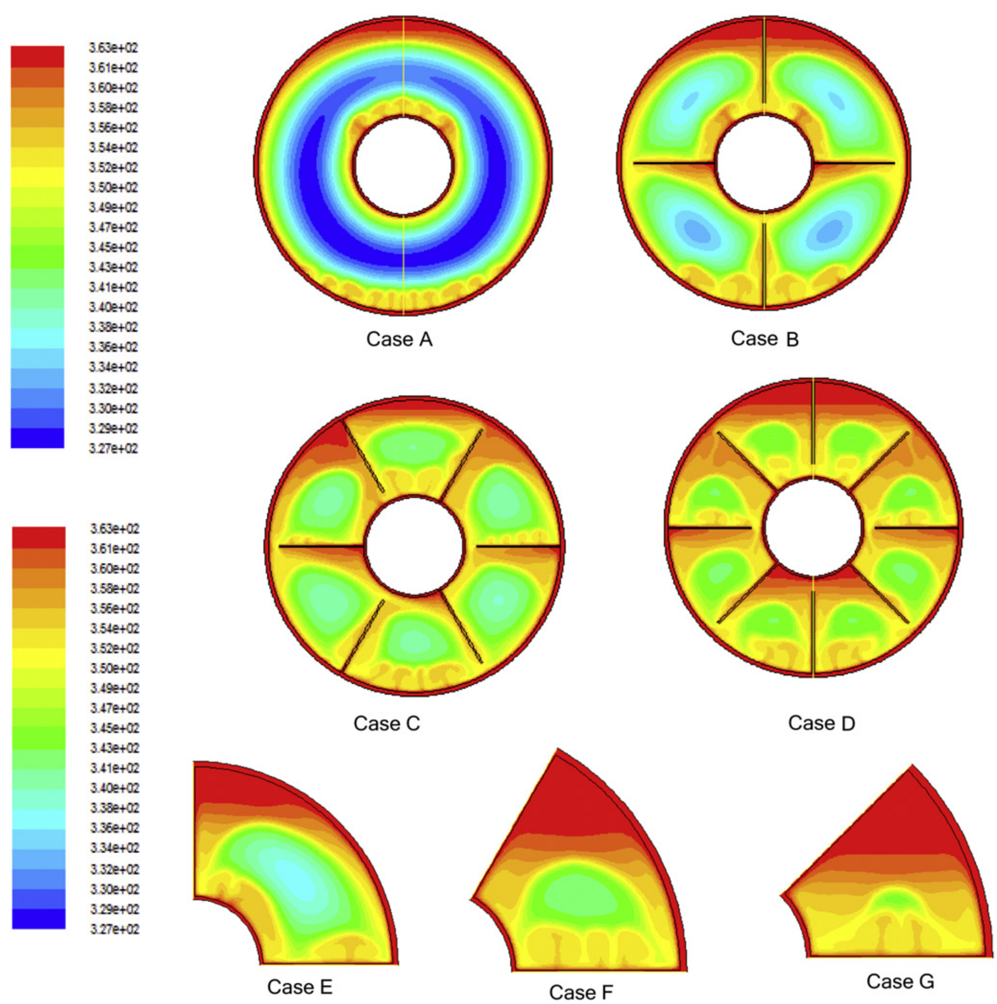

Fig. 13. All cases temperature distribution of TTHX after 30 min.

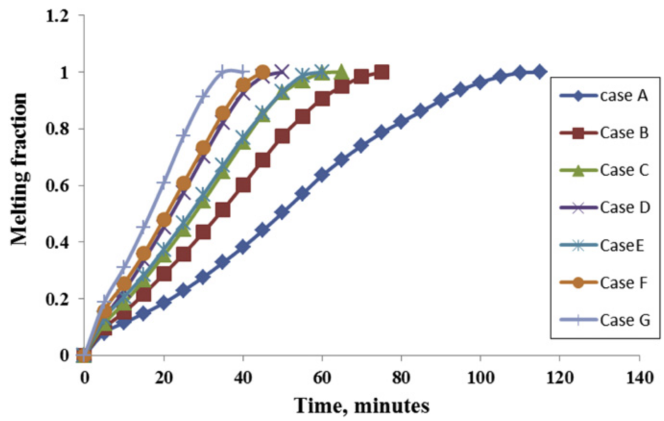

Fig. 14. The melting fraction for all enhancement cases.

4.4. The effect of Stefan number on the melting fraction

Fig. 12 represents the melting fraction versus time for three Stefan numbers of 0.034, 0.057, and 0.09 (temperature difference of 3 °C, 5 °C, and 8 °C, respectively), which describes the operating condition during the melting process in TTHX. The surface temperature T directly affects the value of the Stefan number and is defined as:

$$\mathrm{Ste} = \frac{c_{pl}(T - T_m)}{L} \tag{12}$$

where Cpl is the specific heat of the liquid PCM, L is the latent heat of PCM and Tm is the melting temperature of PCM, a higher surface temperature gives rise to a higher Stefan number. As can be seen in Fig. 12, the difference between the surface temperature and the melting temperature of the PCM affected the melting rate; the higher the temperature difference, the more rapid the increase of the melting fraction, and the shorter the melting rate.

Temperature changes of the PCM inside the TTHX unit after a half-hour of melting for the different cases included in this work were seen in more detail on the contours represents the temperature distributions, as shown in Fig. 13. The heat transfer occurred between the hot wall of the tubes and the solid surface of the PCM by conduction, which dominated the melting at the early stage of melting and caused a thin layer of liquid to form due to the heat-transfer phenomena. As the time progressed, this layer expanded and the liquid fraction increased; the hotter liquid of the PCM was pushed upward to the top of the tubes due to the natural convection effects driven by buoyancy, whereas the solid part of the PCM squeezed down to the bottom of the tube by its heavier density. Fig. 13 indicated the temperature distribution after half-hour of melting for all cases; the natural convection led to an increase in the temperature rate in the upper part of case A whereas the lower part was at lower value. By adding the fins to the TTHX, the transfer of the hotter liquid to the upper part of the TTHX was decreased. As the number of fins increases the natural convection affected the melting in different parts of the PCM, causing a uniform temperature distribution. Complete melting was achieved in case G, where other models took a longer time to finish the melting process.

Fig. 14 shows the melting fraction for all cases. While case A achieved a total complete melting in 115 min, there were a big enhancements for the other cases; as the fins increase, the time required for melting decreases, and the PCM unit geometry with 8-cells completed the melting process of the PCM in around 40 min; In general, it can be concluded that the melting fraction is significantly accelerated by adding internal and external fins to the TTHX, this is because the fins extend the heat transfer area and conduct it directly to the PCM surface.

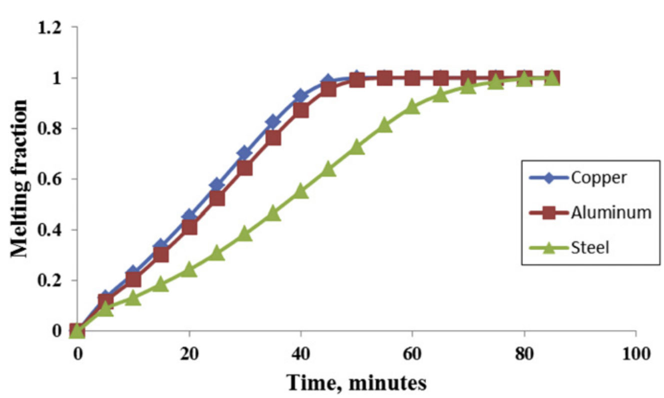

Fig. 15. TTHX material effect on the melting time.

Table 8
Thermo-physical properties of the copper, aluminum, and steel.

Property	Copper	Aluminium	Steel
Density of PCM, solid, ρ_s (kg/m^3)	8978	2719	8030
Specific heat of PCM, solid Cp_s (J/kg K)	381	871	502.48
Thermal conductivity, solid, k (W/m K)	387.6	202.4	16.27

4.5. Effect of TTHX material on the melting fraction

The influence of the material of the TTHX on the melting fraction is shown in Fig. 15 the material investigated were copper, aluminum, and steel for case D. Thermal conductivities of TTHX materials are given in Table 8 as defined in FLUENT software. Comparing the results for copper and aluminum, there was no significant difference in the melting time of the PCM. Steel material consumed longer time to complete the melting of the PCM with respect to the previous materials. Steel material showed an acceptable melting time when the internal-external fins included to the TTHX. Steel material presents an alternative option in the selection of the TTHX materials due to the low cost and easiness of fabrication.

5. Conclusion

Heat transfer enhancement for a triplex tube heat exchanger by using internal and external fins to accelerate the melting rate of RT82 as a PCM were investigated numerically; different design and operation parameters include the fin length, TTHX materials, number of fins, fin thickness, Stefan number and PCM unit geometry were analyzed. Based on the simulation results, these parameters have a significant influence on the time for complete melting; the effect of fin thickness is small compared to the fin length and number of fins, which have a strong effect on the melting rate time. Different cases were studied, and according to the results, case G achieved the complete melting earlier with respect to other cases. Experiments were conducted to validate the proposed model. Simulated results agree with the experimental results.

Nomenclature

C	Mushy zone constant (kg/m^3 s)
Cp	Specific heat of PCM (J/kg K)
gi	Gravity acceleration in the i-direction (m/s^2)
h	sensible enthalpy (J/kg)

H enthalpy (J/kg)
k thermal conductivity (W/m K)
L latent heat fusion (J/kg)
T Temperature (°C or K)
ui velocity component (m/s)
Si Momentum source term in the i-direction (Pa/m)

Greek letters
ρ fluid density(kg/m^3)
β liquid fraction
μ Dynamic viscosity (kg/m s)

Subscripts
i,j components
ini initial
HTF heat transfer fluid
m melting
ref reference
s solidus of the phase change material
l liquidus of the phase change material
t time

References

[1] A.A. Al-Abidi, S. Bin Mat, K. Sopian, M.Y. Sulaiman, C.H. Lim, A. Th, Review of thermal energy storage for air conditioning systems, Renewable and Sustainable Energy Reviews 16 (2012) 5802–5819.
[2] A. Pasupathy, L. Athanasius, R. Velraj, R.V. Seeniraj, Experimental investigation and numerical simulation analysis on the thermal performance of a building roof incorporating phase change material (PCM) for thermal management, Applied Thermal Engineering 28 (2008) 556–565.
[3] P. Meshgin, Y. Xi, Y. Li, Utilization of phase change materials and rubber particles to improve thermal and mechanical properties of mortar, Construction and Building Materials 28 (2012) 713–721.
[4] A.M. Borreguero, M. Luz Sánchez, J.L. Valverde, M. Carmona, J.F. Rodríguez, Thermal testing and numerical simulation of gypsum wallboards incorporated with different PCMs content, Applied Energy 88 (2011) 930–937.
[5] A. Joulin, Z. Younsi, L. Zalewski, S. Lassue, D.R. Rousse, J.-P. Cavrot, Experimental and numerical investigation of a phase change material: thermal-energy storage and release, Applied Energy 88 (2011) 2454–2462.
[6] J. Bony, S. Citherlet, Numerical model and experimental validation of heat storage with phase change materials, Energy and Buildings 39 (2007) 1065–1072.
[7] L.F. Cabeza, M. Ibáñez, C. Solé, J. Roca, M. Nogués, S. Hiebler, H. Mehling, Use of phase-change materials in solar domestic hot water tanks, ASHRAE Transactions 112 (1) (2006) 495–508.
[8] V. Shatikian, G. Ziskind, R. Letan, Numerical investigation of a PCM-based heat sink with internal fins: constant heat flux, International Journal of Heat and Mass Transfer 51 (2008) 1488–1493.
[9] Y.-H. Wang, Y.-T. Yang, Three-dimensional transient cooling simulations of a portable electronic device using PCM (phase change materials) in multi-fin heat sink, Energy 36 (2011) 5214–5224.
[10] G. Çakmak, C. Yıldız, The drying kinetics of seeded grape in solar dryer with PCM-based solar integrated collector, Food and Bioproducts Processing 89 (2011) 103–108.
[11] V. Pandiyarajan, M. Chinna Pandian, E. Malan, R. Velraj, R.V. Seeniraj, Experimental investigation on heat recovery from diesel engine exhaust using finned shell and tube heat exchanger and thermal storage system, Applied Energy 88 (2011) 77–87.
[12] E. Oró, L. Miró, M.M. Farid, L.F. Cabeza, Improving thermal performance of freezers using phase change materials, International Journal of Refrigeration 35 (2012) 984–991.
[13] H. Tan, C. Li, Y. Li, Simulation research on PCM freezing process to recover and store the cold energy of cryogenic gas, International Journal of Thermal Sciences 50 (2011) 2220–2227.
[14] A. Mahmud, K. Sopian., M.A. Alghoul, M. Sohif, Using a paraffin wax–aluminum compound as a thermal storage material in solar air heater, Journal of Engineering and Applied Sciences 4 (2009) 74–77.
[15] S.D. Sharma, T. Iwata, H. Kitano, K. Sagara, Thermal performance of a solar cooker based on an evacuated tube solar collector with a PCM storage unit, Solar Energy 78 (2005) 416–426.
[16] F. Agyenim, P. Eames, M. Smyth, Experimental study on the melting and solidification behaviour of a medium temperature phase change storage material (Erythritol) system augmented with fins to power a LiBr/H_2O absorption cooling system, Renewable Energy 36 (2011) 108–117.
[17] A. Erek, Z. Ī1ken, M.A. Acar, Experimental and numerical investigation of thermal energy storage with a finned tube, International Journal of Energy Research 29 (2005) 283–301.
[18] L.F. Cabeza, H. Mehling, S. Hiebler, F. Ziegler, Heat transfer enhancement in water when used as PCM in thermal energy storage, Applied Thermal Engineering 22 (2002) 1141–1151.
[19] Y. Hamada, J. Fukai, Latent heat thermal energy storage tanks for space heating of buildings: comparison between calculations and experiments, Energy Conversion and Management 46 (2005) 3221–3235.
[20] F. Agyenim, P. Eames, M. Smyth, Heat transfer enhancement in medium temperature thermal energy storage system using a multitube heat transfer array, Renewable Energy 35 (2010) 198–207.
[21] R. Velraj, R.V. Seeniraj, B. Hafner, C. Faber, K. Schwarzer, Heat transfer enhancement in a latent heat storage system, Solar Energy 65 (1999) 171–180.
[22] M. Fang, G. Chen, Effects of different multiple PCMs on the performance of a latent thermal energy storage system, Applied Thermal Engineering 27 (2007) 994–1000.
[23] H.A. Adine, H. El Qarnia, Numerical analysis of the thermal behaviour of a shell-and-tube heat storage unit using phase change materials, Applied Mathematical Modelling 33 (2009) 2132–2144.
[24] F. Agyenim, N. Hewitt, P. Eames, M. Smyth, A review of materials, heat transfer and phase change problem formulation for latent heat thermal energy storage systems (LHTESS), Renewable and Sustainable Energy Reviews 14 (2010) 615–628.
[25] K.A.R. Ismail, C.L.F. Alves, M.S. Modesto, Numerical and experimental study on the solidification of PCM around a vertical axially finned isothermal cylinder, Applied Thermal Engineering 21 (2001) 53–77.
[26] F. Agyenim, P. Eames, M. Smyth, A comparison of heat transfer enhancement in a medium temperature thermal energy storage heat exchanger using fins, Solar Energy 83 (2009) 1509–1520.
[27] V. Shatikian, G. Ziskind, R. Letan, Numerical investigation of a PCM-based heat sink with internal fins, International Journal of Heat and Mass Transfer 48 (2005) 3689–3706.
[28] P.V. Padmanabhan, M.V.K. Murthy, Outward phase change in a cylindrical annulus with axial fins on the inner tube, International Journal of Heat and Mass Transfer 29 (1986) 1855–1868.
[29] U. Stritih, An experimental study of enhanced heat transfer in rectangular PCM storage, International Journal of Heat and Mass Transfer 47 (2004) 2841–2847.
[30] R. Velraj, R.V. Seeniraj, B. Hafner, C. Faber, K. Schwarzer, Experimental analysis and numerical modelling of inward solidification on a finned vertical tube for a latent heat storage unit, Solar Energy 60 (1997) 281–290.
[31] M. Medrano, M.O. Yilmaz, M. Nogués, I. Martorell, J. Roca, L.F. Cabeza, Experimental evaluation of commercial heat exchangers for use as PCM thermal storage systems, Applied Energy 86 (2009) 2047–2055.
[32] J.R. Balikowski, J.C. Mollendorf, Performance of phase change materials in a horizontal annulus of a double-pipe heat exchanger in a water-circulating loop, Journal of Heat Transfer 129 (2007) 265–272.
[33] Y. Zhang, A. Faghri, Heat transfer enhancement in latent heat thermal energy storage system by using the internally finned tube, International Journal of Heat and Mass Transfer 39 (15) (1996) 3165–3173.
[34] O. García-Valladares, Numerical simulation of triple concentric-tube heat exchangers, International Journal of Thermal Sciences 43 (2004) 979–991.
[35] A.R. Darzi, M. Farhadi, K. Sedighi, Numerical study of melting inside concentric and eccentric horizontal annulus, Applied Mathematical Modelling 36 (2012) 4080–4086.
[36] A.D. Brent, V.R. Voller, K.J. Reid, Enthalpy–porosity technique for melting convection–diffusion phase change : application to the melting of a pure metal, Numerical Heat Transfer 13 (1988) 297–318.
[37] W.-B. Ye, D.-S. Zhu, N. Wang, Numerical simulation on phase-change thermal storage/release in a plate-fin unit, Applied Thermal Engineering 31 (2011) 3871–3884.
[38] S.V. Patankar (Ed.), Numerical Heat Transfer and Fluid Flow, McGrawHill, NewYork, 1980.
[39] A.A. Al-Abidi, S.B. Mat, K. Sopian, M.Y. Sulaiman, A.T. Mohammed, CFD applications for latent heat thermal energy storage: a review, Renewable and Sustainable Energy Reviews 20 (2013) 353–363.